



Electrochemistry and ion-sensing properties of calix[4]arene derivatives

Shanshan Chen^a, Richard D. Webster^{a,*}, Carmen Talotta^b, Francesco Troisi^b,
Carmine Gaeta^b, Placido Neri^{b,**}

^a Division of Chemistry and Biological Chemistry, School of Physical and Mathematical Sciences, Nanyang Technological University, Singapore 637371, Singapore

^b Dipartimento di Chimica, Università di Salerno, Via Ponte don Melillo, I-84084 Fisciano (Salerno), Italy

ARTICLE INFO

Article history:

Received 24 April 2010

Received in revised form 24 June 2010

Accepted 26 June 2010

Keywords:

Calixarenes

Bromodienone

Polymer membrane ion-selective electrode

Radical cation

Cesium cation

ABSTRACT

The cyclic voltammetric properties of several substituted calix[4]arenes were examined in acetonitrile and dichloromethane. The compounds that contained one phenolic group in the macrocyclic cavity were able to be electrochemically oxidised at positive potentials. In acetonitrile, cyclic voltammetry experiments indicated that the phenolic compounds were oxidised in a two-electron (one-proton) process over all measured scan rates (up to 50 V s^{-1}), while in dichloromethane, the oxidation process occurred by one-electron at scan rates $\geq 5 \text{ V s}^{-1}$, to most likely form the radical cations. In both solvents, longer timescale (minutes to hours) controlled potential coulometry experiments indicated that the oxidation process occurred by two-electrons per molecule, to form reactive diamagnetic cations that could not be reduced back to the starting materials under electrolysis conditions. The ion-sensing properties of the compounds were investigated in polymer membrane ion-selective electrodes and it was found that they responded reversibly in a Nernstian fashion to Groups 1 and 2 metals and had the highest selectivity to the cesium cation.

© 2010 Elsevier Ltd. All rights reserved.

1. Introduction

The supramolecular sensing properties of calixarenes towards ions or neutral molecules have been studied extensively over the last two decades [1–3]. The weak and reversible interactions with Groups 1 and 2 metals have made them ideal for use in potentiometric chemical sensors and in optical sensors [1–3]. Considerable attention has focused on new synthetic strategies to modify the calixarene structures to improve or diversify their recognition properties [4–7]. In this work we discuss the sensing properties of some calix[4]arenes recently synthesised *via* the so-called “*p*-bromodienone route” [8,9], where one aromatic group contains a hydroxyl (phenolic) or quinone [10] based functionality (Scheme 1, compounds **1a**, **1b**, **2a**, **5a**, **5b** and **5c**).

In addition to the ion-sensing properties of the calix[4]arenes, the electrochemical properties were also examined. Calixarenes often display complicated electrochemical properties due to the presence of several phenolic or ether groups resulting in multiple electron transfer oxidative processes, and because of adsorption processes affecting the shape of the voltammograms [11–14]. Usually the calixarenes with phenolic or ether groups display a multi-electron oxidation process at potentials $\geq 1 \text{ V vs. ferrocene}^{0/+}$

(Fc/Fc⁺), with the cyclic voltammograms displaying a forward oxidation peak but no reverse reductive peak when the scan direction is switched, indicating that the oxidised compounds undergo coupled chemical reactions after the initial electron transfer step [11–14]. However, compounds **1a**, **5a**, **5b** and **5c** contain one electroactive phenolic group, and so were expected to show simpler electrochemical properties. Phenolic compounds are known to undergo a number of proton and electron transfer reactions in an electrochemical “square-scheme” mechanism, where the lifetimes of the oxidised species depend on their structures and particularly on the substituents in the 2, 4 and 6 positions [15–18]. Recent studies have demonstrated that some phenolic compounds can be oxidised to form relatively long-lived diamagnetic cations (phenoxonium ions) in a two-electron and one-proton process [19–28]. We were particularly interested in determining whether the macrocyclic structure of the calix[4]arenes, composed by electron-rich π -basic rings, could impact improved lifetimes on the oxidised forms of their phenolic rings.

2. Experimental

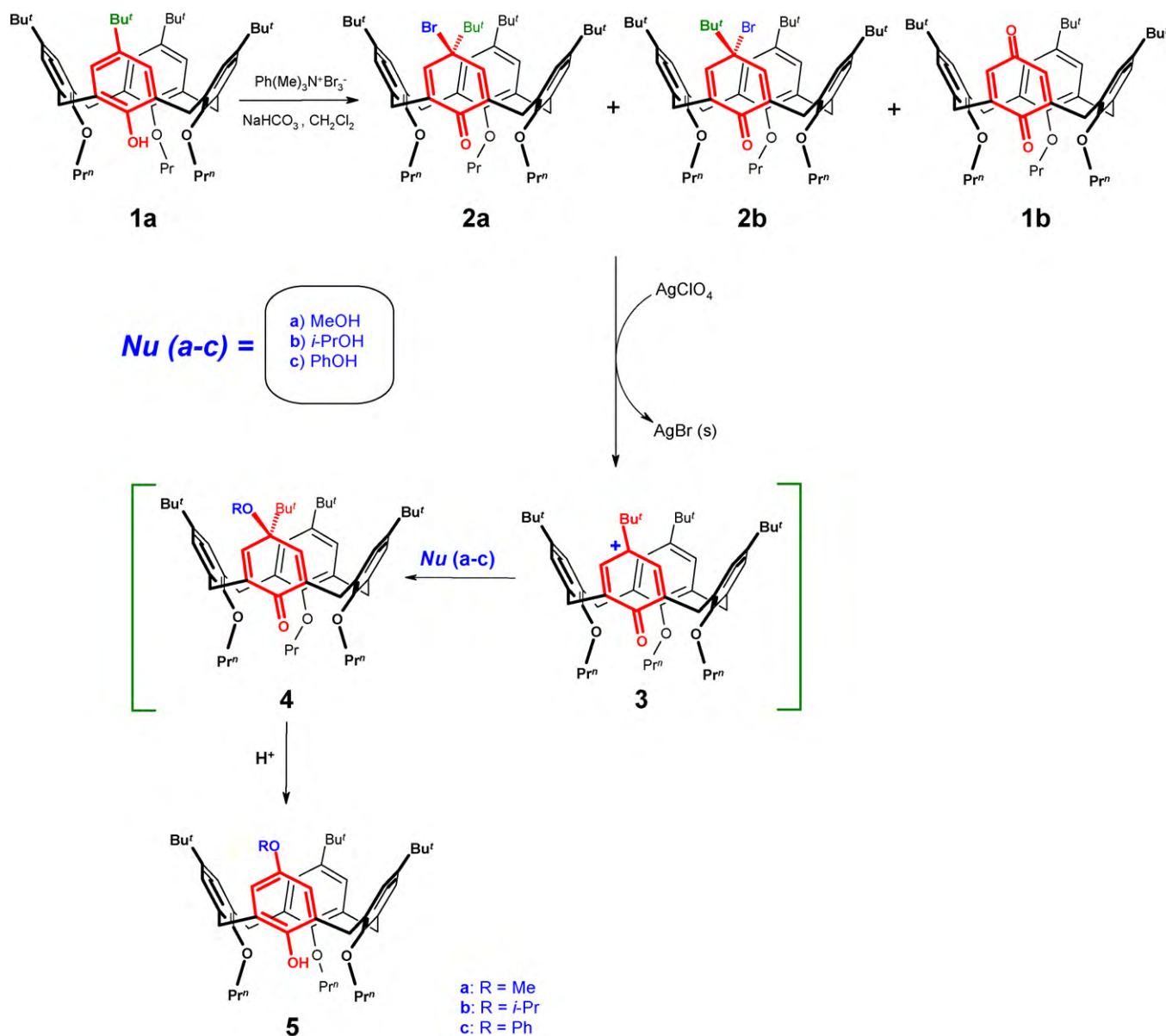
2.1. Chemicals and reagents

HPLC grade CH₃CN (Tedia) and CH₂Cl₂ (J.T. Baker) were dried over 3 Å molecular sieves and HPLC grade tetrahydrofuran (THF) was used directly from the bottle. Bu₄NPF₆ was prepared by reacting equal molar amounts of aqueous solutions of Bu₄NOH

* Corresponding author. Tel.: +65 6316 8793; fax: +65 6791 1961.

** Corresponding author. Tel.: +39 089 969572; fax: +39 089 969603.

E-mail addresses: webster@ntu.edu.sg (R.D. Webster), neri@unisa.it (P. Neri).



Scheme 1. Structure of compounds and the synthetic *p*-bromodienone route.

(40%, Alfa Aesar) and HPF_6 (65%, Fluka), washing the precipitate with hot water, recrystallising 3 times from hot ethanol followed by drying under vacuum at 160°C for 24 h and storing under vacuum. High molecular weight poly(vinyl chloride), 2-nitrophenyl octyl ether (NPOE) and potassium tetrakis(4-biphenyl)borate (KTBPB) were obtained from Fluka. Di-*n*-octyl phenylphosphonate (DOPP), di-*n*-butyl sebacate (DBS), di-*n*-butyl phthalate (DBP) were obtained from Alfa Aesar. LiCl, NaCl, KCl, CsCl, CaCl_2 , NH_4Cl , MgSO_4 salts were obtained from Goodrich Chemical Enterprise (GCE). Rb^+ standard solution (1000 $\mu\text{g}/\text{ml}$ in 2% HNO_3) was obtained from Certified standards. All sample solutions for analysis were prepared with water, with a resistivity $\geq 18\text{ M}\Omega\text{ cm}$ from an ELGA Purelab Option-Q. The synthesis of compounds **1a**, **1b**, **2a**, **5a**, **5b** and **5c** has been described previously [8,10].

2.2. Voltammetry

Cyclic voltammetry (CV) experiments were conducted with a computer controlled Eco Chemie $\mu\text{Autolab III}$ potentiostat. Working electrodes were 1 mm diameter planar Pt and glassy carbon

(GC) disks (Cypress Systems), used in conjunction with a Pt auxiliary electrode (Metrohm) and an Ag wire miniature reference electrode (Cypress Systems) connected to the test solution via a salt bridge containing 0.5 M Bu_4NPF_6 in CH_3CN . Accurate potentials were obtained using ferrocene as an internal standard, which was added to the test solution at the end of the measurements.

2.3. Controlled potential electrolysis

Bulk electrolysis experiments were performed in a divided controlled potential electrolysis (CPE) cell separated with a porosity no. 5 (1.0–1.7 μm) sintered glass frit [29]. The working and auxiliary electrodes were identically sized Pt mesh plates symmetrically arranged with respect to each other with an Ag wire reference electrode (isolated by a salt bridge) positioned to within 2 mm of the surface of the working electrode. The volumes of both the working and auxiliary electrode compartments were approximately 20 ml each. The solution in the working electrode compartment was simultaneously deoxygenated and stirred using bubbles of argon gas. The number of electrons (n) transferred

during the bulk oxidation process was calculated from

$$N = \frac{Q}{nF} \quad (1)$$

where N is the no. of moles of starting compound, Q is the charge (coulombs) and F is Faraday constant ($96,485 \text{ C mol}^{-1}$).

2.4. Preparation of polymer membrane ion-selective electrodes

The PVC-based membranes were prepared by mixing the calix[4]arenes (1 mg), KTBPB (1 mg), plasticizers (65 mg), and PVC (33 mg) in THF (2 ml). After the mixture had completely dissolved in the THF, the clear solution was poured into a 5 cm diameter Petri dish and the THF was allowed to evaporate for approximately 24 h at room temperature. A 5 mm diameter circular piece of the membrane was cut out and attached to the end of a commercial electrode (Selectophore Fluka). The inner filling solution of the ISE electrode contained 0.1 M of the ions that the electrode was tested with, and the electrode/membrane was conditioned for 2 days in a 0.5 M solution of the particular ion.

2.5. Selectivity coefficient measurements

Selectivity coefficients (K_{ij}^{pot}) were determined using cesium as the primary ion (i) and other Groups 1 and 2 metals as interfering ions (j) using both the fixed interference method (FIM) and separate solution method (SSM) [30–33]. In the SSM, the solution of 0.01 M NaCl served as the internal filling solution and the electrodes were conditioned in 0.01 M NaCl solution for at least 48 h before measuring other 0.01 M interfering ions and 0.01 M primary cesium ion. The selectivity coefficient was calculated by Eq. (2), where E_i is the cell potential of the solution containing the primary ion, E_j is the cell potential of the solution containing the interfering ion, Z_i and Z_j are the charges on the primary and interfering ions respectively, a_i is the activity of the primary ion calculated by Debye–Hückel theory, R is the gas constant ($8.3143 \text{ J K}^{-1} \text{ mol}^{-1}$), T is the temperature (in K) and F is Faraday constant ($96,485 \text{ C mol}^{-1}$):

$$\log K_{ij}^{\text{pot}} = \frac{E_j - E_i}{(2.303RT)/(Z_i F)} + \left(1 - \frac{Z_i}{Z_j}\right) \log a_i \quad (2)$$

For the FIM, the concentration of the interfering ion was kept at 0.01 M, whereas the Cs^+ ion was varied from 1.0×10^{-7} to 1.0×10^{-1} M. Before taking any potential measurements, the membranes were equilibrated in 0.5 M Cs^+ solution for 48 h, and the inner solution consisted of 0.1 M CsCl. The selectivity coefficients were calculated from Eq. (3), where DL (detection limit) and BG (background) were obtained graphically from readings of the primary ion in the presence of the interfering ion [33]:

$$\log K_{ij}^{\text{pot}} = \log \frac{a_i(\text{DL})}{a_j(\text{BG})^{Z_i/Z_j}} \quad (3)$$

3. Results and discussion

3.1. Electrochemistry of monophenolic calix[4]arenes **1a**, **5a**, **5b**, and **5c**

Fig. 1a shows CVs of *p*-methoxyphenolic calix[4]arene (**5a**) in CH_3CN at a variety of scan rates at a GC electrode. The compound shows an oxidation process with an anodic peak potential (E_p^{ox}) at $\sim +0.6 \text{ V vs. Fc/Fc}^+$. The oxidation process remained chemically irreversible in the sense that the anodic (i_p^{ox}) to cathodic (i_p^{red}) peak current ratio ($i_p^{\text{ox}}/i_p^{\text{red}}$) was $\gg 1$ at all measured scan rates (Fig. 1a). The reason for the chemical irreversibility in the CVs relates to a coupled chemical reaction that occurs after the initial electron

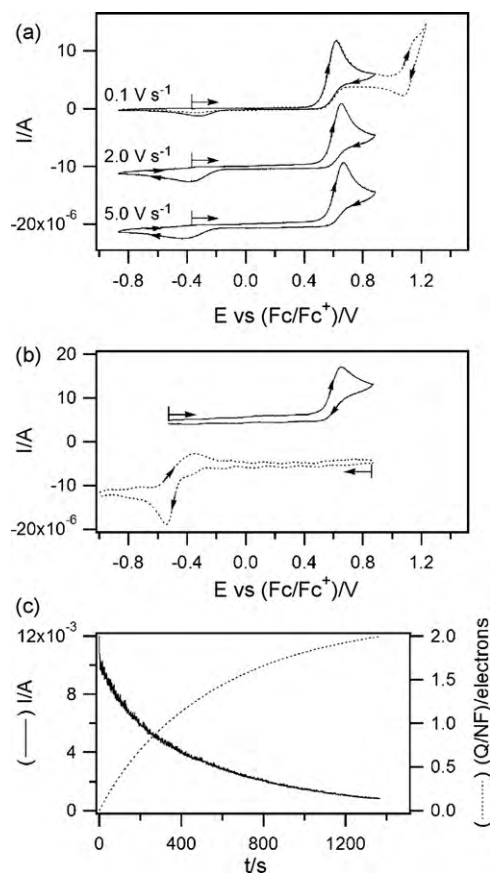


Fig. 1. Voltammetric and coulometric data of 1 mM **5a** in CH_3CN with 0.2 M Bu_4NPF_6 . (a) CVs recorded at $22 \pm 2^\circ\text{C}$ at variable scan rates with a 1 mm diameter GC electrode. Current data were scaled by multiplying by $\nu^{-0.5}$. (b) CVs recorded at $-20 \pm 2^\circ\text{C}$ at a 1 mm diameter Pt electrode (solid line) prior to the bulk oxidation of **5a**, and (dotted line) after the exhaustive oxidation of **5a** at an applied potential of +0.8 V vs. Fc/Fc^+ . Current data were scaled by multiplying by $\nu^{-0.5}$. (c) Current/coulometry vs. time data obtained during the exhaustive oxidation of **5a** at +0.8 V vs. Fc/Fc^+ at $-20 \pm 2^\circ\text{C}$.

transfer step (an EC or ECE process), and not due to a slow heterogeneous electron transfer rate. It is possible that if sufficiently fast scan rates were used in CH_3CN , the $i_p^{\text{ox}}/i_p^{\text{red}}$ -ratio could approach unity (if the follow up homogeneous reaction was outrun) [34].

In contrast to the data in CH_3CN , the CV data obtained in CH_2Cl_2 show that the $i_p^{\text{ox}}/i_p^{\text{red}}$ -ratio for the first oxidation process approaches unity as the scan rate is increased to 5 V s^{-1} (Fig. 2a). Furthermore, the anodic (E_p^{ox}) to cathodic (E_p^{red}) peak-to-peak potential separation ($\Delta E_{\text{pp}} = 100 \text{ mV}$) at the fastest scan rate (5 V s^{-1}) was the same as the value observed for ferrocene (a model system for fast electron transfer [35]) under the same conditions, indicating that the cyclic voltammograms for **5a** were not affected by slow heterogeneous electron transfer rates. The ΔE_{pp} -value of 100 mV at a scan rate of 5 V s^{-1} is wider than the theoretical value of 57 mV at 25°C for a one-electron transfer [34], but this likely originates from uncompensated solution resistance effects brought about by the low dielectric constant of CH_2Cl_2 ($\epsilon = 9.1$). When the concentration of **5a** was decreased to 0.2 mM, the ΔE_{pp} -value obtained by CV at 5 V s^{-1} decreased to 75 mV, which supports the larger than theoretical value of ΔE_{pp} being due to solution resistance effects. The data in Fig. 2a show that the anodic peak current (i_p^{ox}) is proportional to the square root of the scan rate, which is the expected result for a diffusion controlled process [34].

The oxidation of phenols (POH) typically occurs by two-electrons per molecule *via* an electrochemical ECE mechanism (Scheme 2) [15–28], or possibly *via* a disproportionation mecha-

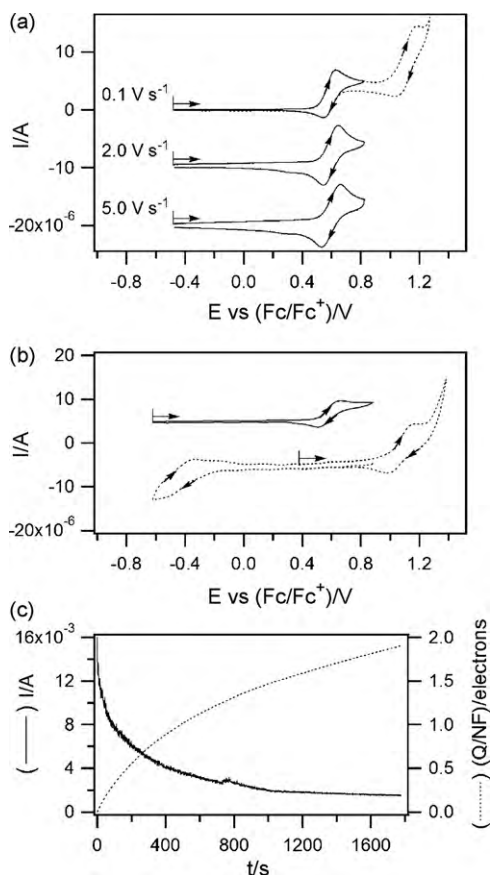


Fig. 2. Voltammetric and coulometric data of 1 mM **5a** in CH_2Cl_2 with 0.2 M Bu_4NPF_6 . (a) CVs recorded at $22 \pm 2^\circ\text{C}$ at variable scan rates with a 1 mm diameter GC electrode. Current data were scaled by multiplying by $\nu^{-0.5}$. (b) CVs recorded at $-20 \pm 2^\circ\text{C}$ at a 1 mm diameter Pt electrode (solid line) prior to the bulk oxidation of **5a**, and (dotted line) after the exhaustive oxidation of **5a** at an applied potential of $+0.8\text{ V vs. Fc/Fc}^+$. Current data were scaled by multiplying by $\nu^{-0.5}$. (c) Current/coulometry vs. time data obtained during the exhaustive oxidation of **5a** at $+0.8\text{ V vs. Fc/Fc}^+$ at $-20 \pm 2^\circ\text{C}$.

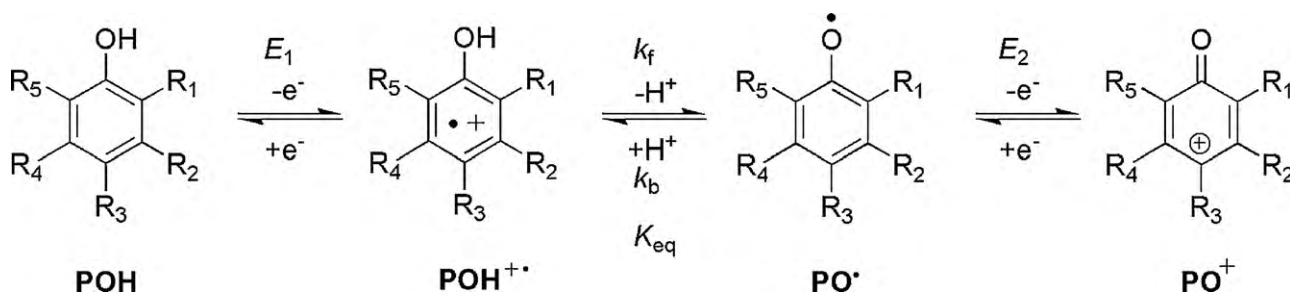
nism that also involves two-electrons per molecule [26]. The first electron transfer step produces the cation radical ($\text{POH}^{+\bullet}$), which loses a proton to form a neutral phenoxyl radical (PO^\bullet). Because the phenoxyl radicals are easier to oxidise than their associated phenols, they immediately undergo further oxidation to form the diamagnetic cation (PO^+). Normally the diamagnetic cations are short-lived and undergo rapid hydrolysis reactions with trace water or other nucleophiles in the solvent [15–28].

The cyclic voltammograms obtained in CH_3CN (Fig. 1a) which show $i_p^{\text{ox}}/i_p^{\text{red}}$ -ratios $\gg 1$ at all scan rates are consistent with what is expected for most phenols, where the oxidation mechanism occurs by two-electrons per molecule in a chemically irreversible process. However, the voltammograms that are observed in CH_2Cl_2

(Fig. 2a) are similar in appearance to what is expected for a one-electron transfer. Therefore, it is likely that the difference in the CVs observed in the two solvents is due to a different number of electrons transferred on the short voltammetric timescale (seconds). It was previously observed that the cation radical of the phenolic compound α -tocopherol had an increased lifetime in CH_2Cl_2 compared to in CH_3CN , due to a change in the equilibrium constant for the deprotonation step of the cation radical (K_{eq} in Scheme 2) [20–25,36]. This can be rationalised by the phenolic radical cations being less acidic in low dielectric constant solvents. It is likely that the same situation applies to **5a**, so that the cation radical formed by initial one-electron oxidation has a longer lifetime in CH_2Cl_2 compared to CH_3CN . The CVs obtained of **5a** in CH_2Cl_2 display lower peak currents than those obtained for equivalent concentrations in CH_3CN , which supports the assignment of the one-electron oxidation in CH_2Cl_2 (assuming similar diffusion coefficient values between the different solvents).

An alternative mechanism to account for the $i_p^{\text{ox}}/i_p^{\text{red}}$ -ratio of unity for the CV of **5a** at a scan rate of 5 V s^{-1} in CH_2Cl_2 (Fig. 2a), involves the reversible two-electron/one-proton process given in Scheme 2 to produce a diamagnetic cation (an ECE mechanism), as seen for α -tocopherol [20–25]. It can be proposed that the forward oxidative CV scan produces the diamagnetic cation (PO^+) and the reverse reductive scan regenerates the starting material (POH). However, this reversible two-electron process is considered unlikely for compound **5a**. In situations where a diamagnetic cation has been voltammetrically detected, the E_p^{ox} to E_p^{red} separations (ΔE_{pp}) are usually very wide (~ 300 – 400 mV) due to the wide potential separation between the formal potentials (E_f^0) of the phenol and phenoxyl ion oxidation steps (E_1 and E_2 in Scheme 2). The ΔE_{pp} -value of 100 mV observed in the CV in Fig. 2a at a scan rate of 5 V s^{-1} , is instead consistent with a one-electron transfer, taking into account the resistance effects of the low dielectric constant solvent.

Although the cyclic voltammograms in CH_2Cl_2 (Fig. 2a) show signs of chemical reversibility, the observation that scan rates $> 0.1\text{ V s}^{-1}$ are needed to obtain $i_p^{\text{ox}}/i_p^{\text{red}}$ -ratios approaching unity, indicates that the lifetime of the one-electron oxidised species is still only a few seconds. Controlled potential electrolysis of **5a** in both CH_3CN (Fig. 1c) and CH_2Cl_2 (Fig. 2c) occurred by the transfer of close to two-electrons per molecule. Therefore, the longer timescale electrolysis experiments in CH_2Cl_2 allow time for the intermediate cation radical to undergo deprotonation and then be further oxidised, resulting in an increase in the number of electrons transferred compared to the faster timescale CV experiments. It was also observed that in both exhaustively electrolysed solutions (CH_2Cl_2 and CH_3CN), the two-electron oxidised compound had reacted to form a new product that showed a reduction process at approximately -0.4 to $-0.6\text{ V vs. Fc/Fc}^+$ (Figs. 1b and 2b), indicating that the diamagnetic cation (if formed) was not long-lived under electrolysis conditions. During the electrolysis reaction the solution was observed to change to a pale yellow-green colour, possibly due to the appearance of the intermediate radical cation



Scheme 2. Oxidation mechanism for phenols [15–28].

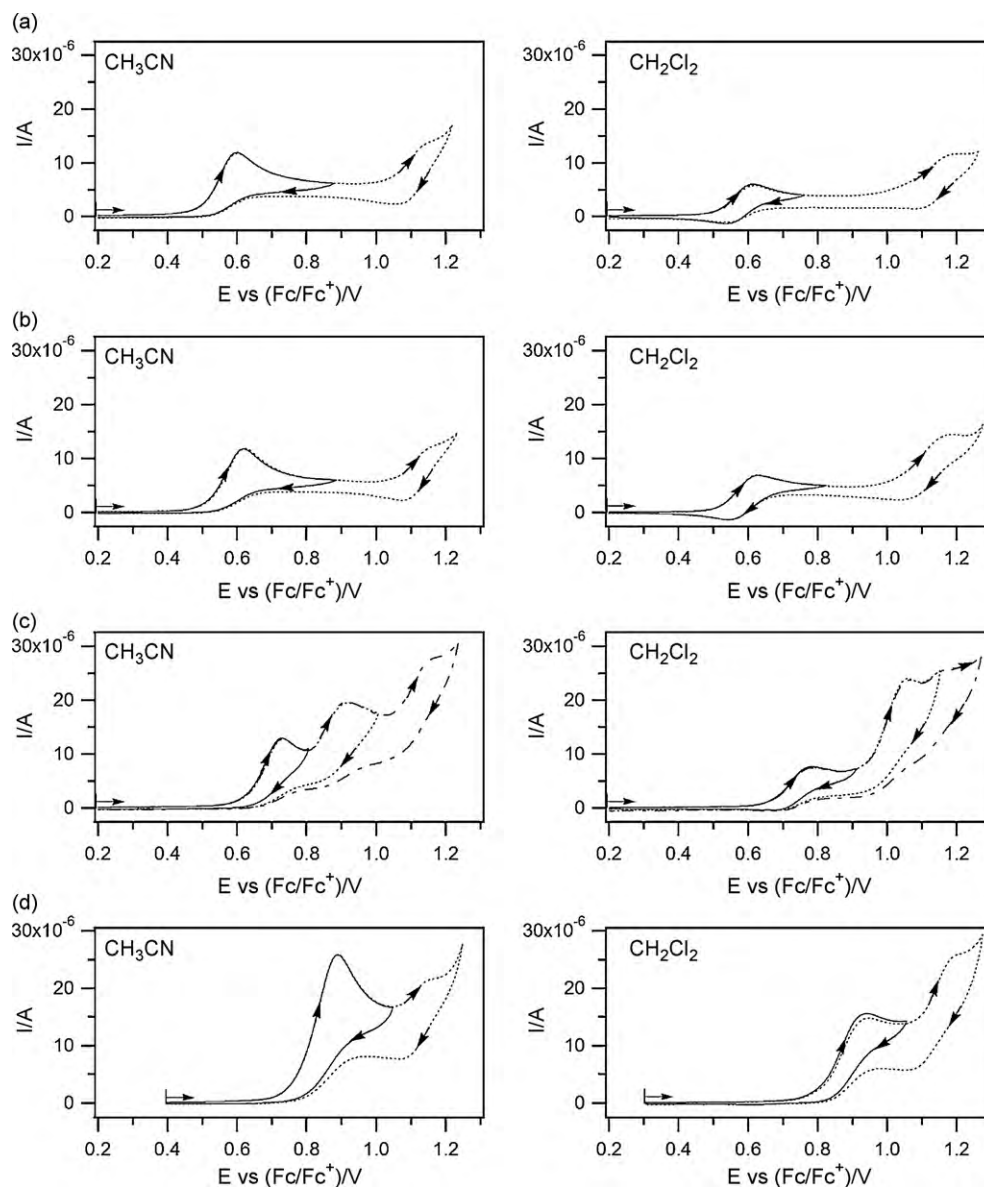


Fig. 3. CVs obtained at $T = 22 \pm 2^\circ\text{C}$ of 1 mM solutions of analytes recorded at a 1 mm diameter GC working electrode at $\nu = 0.1\text{ V s}^{-1}$ in CH_3CN or CH_2Cl_2 with 0.2 M Bu_4NPF_6 as the supporting electrolyte. Current data were scaled by multiplying by $\nu^{-0.5}$. (a) **5b**, (b) **5a**, (c) **5c** and (d) **1a**.

present in small amounts. The proton released during the oxidation process was not detected at Pt or GC electrodes, although this is consistent with the results obtained during the oxidation of other phenols at Pt surfaces in organic solvents [19–28].

The voltammetric data obtained for phenolic calix[4]arenes *para*-substituted with an *i*-propoxy (**5b**), or phenyloxy (**5c**) group were similar to that obtained for **5a**, although there were some differences in the observed potential of the oxidation processes and the degree of chemical reversibility in CH_2Cl_2 . A comparison of the cyclic voltammetry for each compound in CH_3CN and CH_2Cl_2 is given in Fig. 3. In each case and at the equivalent scan rate, the $i_p^{\text{ox}}/i_p^{\text{red}}$ -ratios were closer to unity in CH_2Cl_2 compared to in CH_3CN , indicating that the homogeneous chemical reactions coupled to the electron transfer steps occurred at a slower rate in CH_2Cl_2 compared to in CH_3CN . As the scan rate was increased, the $i_p^{\text{ox}}/i_p^{\text{red}}$ -ratios for the least positive process observed by cyclic voltammetry in CH_2Cl_2 became very close to unity indicating that the cation radicals had an observable lifetime. In contrast, in CH_3CN , the CVs displayed $i_p^{\text{ox}}/i_p^{\text{red}} \gg 1$ at all scan rates measured (up to 50 V s^{-1}), indicating that the cation radicals formed by the initial

one-electron oxidation were relatively short-lived. Furthermore, in each case the i_p^{ox} -values measured in CH_3CN were significantly larger than those measured in CH_2Cl_2 suggesting a greater number of electrons were transferred in CH_3CN , at least on the short CV timescale. However, longer timescale electrolysis experiments on the *p*-*i*-propoxy derivative (**5b**) in CH_2Cl_2 and CH_3CN at -20°C , indicated in both solvents that the oxidation processes occurred by two-electrons per molecule to form a final product that could not be reduced back to the starting material by applying a reductive potential (similar to the results obtained for **5a**).

The anodic peak current observed for **1a** (with a *t*-butyl group) was greater than the other compounds and the oxidation potential was shifted to more positive potentials (compared to **5a**, **5b** and **5c**). If it is assumed that the diffusion coefficient of **1a** is the same as the other compounds, the increase in peak current for **1a** is likely due to an increased number of electrons transferred. It is possible that the compounds undergo oxidation at multiple sites on the molecule, such as at the ether groups in addition to the phenolic groups. Other calixarenes that do not contain phenolic groups have been reported to undergo chemically irreversible oxidation reactions

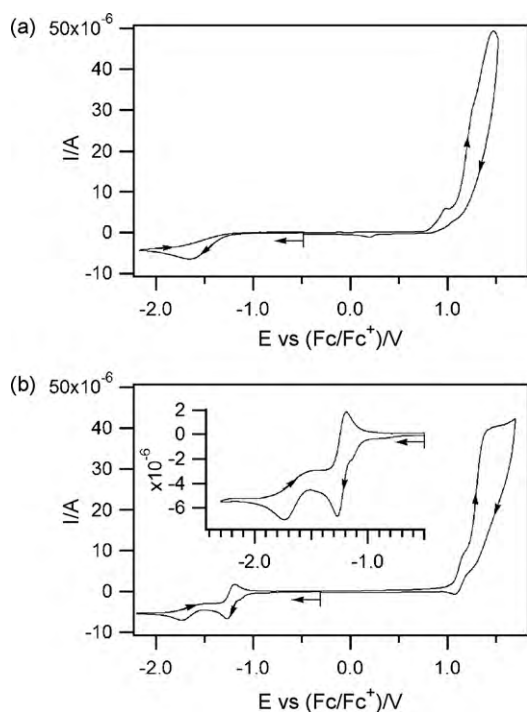


Fig. 4. CVs recorded at a 1 mm diameter GC working electrode at $\nu=0.1 \text{ V s}^{-1}$ and at $22 \pm 2^\circ \text{C}$. Current data were scaled by multiplying by $\nu^{-0.5}$. (a) 1 mM **2a** in CH_2Cl_2 containing 0.2 M Bu_4NPF_6 and (b) 1 mM **1b** in CH_3CN containing 0.2 M Bu_4NPF_6 .

involving multiple electron transfer steps at positive potentials [11,12]. The possibility that the molecules undergo oxidation at more than one site on the molecule is supported by the controlled potential electrolysis data from **5a** (Fig. 2b), where the second oxidation process at approximately +1.1 V vs. Fc/Fc^+ was still detected after the compound had been exhaustively oxidised at +0.8 V vs. Fc/Fc^+ , suggesting that the two processes occurred independently of one another.

3.2. Electrochemistry of calix[4]arene *p*-bromodienone **2a**

A cyclic voltammogram of **2a** in CH_2Cl_2 at 20°C is shown in Fig. 4a, which displays a reduction process at approximately -1.6 V vs. Fc/Fc^+ and a number of oxidation processes at potentials $>+0.9 \text{ V}$ vs. Fc/Fc^+ . The $i_p^{\text{ox}}/i_p^{\text{red}}$ -ratios obtained by cyclic voltammetry for both the oxidation and reduction processes did not show any sign of approaching unity as the scan rate was increased up to 50 V s^{-1} , indicating that the oxidised and reduced forms of **2a** were chemically short-lived. According to the *p*-bromodienone route [8,9], **2a** is thought to convert to compounds **5a**, **5b** and **5c** in an $\text{S}_{\text{N}}1$ mechanism involving the diamagnetic cationic intermediate, **3** (Scheme 1) [8]. Therefore, we were interested in determining whether the intermediate, **3**, could be voltammetrically detected during the oxidation of **2a** with AgSbF_6 (or AgClO_4). **2a** is poorly soluble in CH_3CN but dissolves completely in CH_2Cl_2 . Chemical oxidation experiments were performed by adding equal molar amounts of AgSbF_6 to solutions of **2a** at -25°C in CH_2Cl_2 . Cyclic voltammetry experiments on the chemically oxidised solutions did not show any clear evidence of the presence of an intermediate or semi-stable cation (**3**) that should form *via* loss of the Br^- from the starting material, suggesting that **3** was short-lived (should it actually exist).

3.3. Electrochemistry of calix[4]arene monoquinone **1b**

Cyclic voltammetry experiments on **1b** in CH_3CN led to the detection of two reduction processes at approximately -1.2 and

-1.8 V vs. Fc/Fc^+ (Fig. 4b). The first reduction process at -1.2 V vs. Fc/Fc^+ had an $i_p^{\text{ox}}/i_p^{\text{red}}$ -ratio close to unity at slow scan rates ($\nu=0.1 \text{ V s}^{-1}$), indicating that the reduced species survived on the timescale of the CV experiment. The ΔE_{pp} -value obtained by CV for the first reduction process was 65 mV, suggesting a one-electron process to most likely form an anion radical. Coulometry experiments performed by exhaustively reducing **1b** in CH_3CN in an electrolysis cell at -1.5 V vs. Fc/Fc^+ confirmed the transfer of one-electron per molecule over electrolysis timescales. However, the anion radical did not survive for a sufficiently long time to enable it to be oxidised back to the starting material, and most likely underwent further chemical reactions. There is also a pre-peak or shoulder before the first reduction process in Fig. 4b at approximately -1.1 V vs. Fc/Fc^+ which has not been assigned.

The second reductive electron transfer process at -1.8 V vs. Fc/Fc^+ in Fig. 4b only displayed a forward reduction peak ($E_{\text{p}}^{\text{red}}$) with no detectable oxidation peak (E_{p}^{ox}) when the scan direction was reversed. The i_p^{red} -value for the second electron transfer process was much less than the first process (Fig. 4b). In organic solvents, quinones are often reduced in two one-electron steps to form first the anion radical (semiquinone) and then at more negative potentials the dianion is produced [37–41]. However, it is not clear whether the second electron transfer step that occurs at -1.8 V vs. Fc/Fc^+ is due to the further reduction of the semiquinone, or due to a different electron transfer process. It can be observed in Fig. 4a that compound **2a**, which does not contain a quinone group, also shows a reduction process at -1.6 V vs. Fc/Fc^+ which is similar in appearance to the process observed for **1a**.

The cyclic voltammetric results that were obtained for **2a** and **1b** (Fig. 4) indicate that the compounds can also be oxidised but at a greater potential than the other compounds shown in Fig. 3. Furthermore, the oxidation peak currents for **2a** and **1b** were greater than the other compounds indicating that multiple electron steps were occurring. The major difference between **2a/1b** and the other compounds is that they do not contain a phenolic group. Therefore, it is likely that the oxidation for **2a** and **1b** is associated with the ether groups as has been observed for other calixarenes that display multiple electron transfer processes at potentials $>+1 \text{ V}$ [11,12].

3.4. Ion-sensing properties

The sensing properties of the compounds were tested for Groups 1 and 2 ions by incorporating the molecules into polymer membrane ion-selective electrodes (see Section 2) [42–50]. The membrane composition consisted (by mass) of PVC (33%), several different types of plastizers (65%), potassium tetrakis-(4-biphenyl)borate as the counter ion (1%) and the calix[4]arene (1%). A total ionic strength adjustment buffer was not used for the measurements because of strong interference from the Groups 1 and 2 metals commonly used in buffers.

The membranes containing the sensing compounds were all found to display a potential dependent response except for the membrane containing *p*-bromodienone **2a** (and **2b**), which showed no change in potential as the concentration of ions were varied. **2a** has a bromide and a *tert*-butyl group bonded to the same carbon, which could hinder ions entering the calix[4]arene cavity from the *upper* or *wide* (or *exo*) rim, thereby preventing weak bonding interactions. However, it is more likely that the cations interact with the O-atoms on the lower rim, therefore; **2a** should offer similar ion-sensing properties to the other compounds. There are several reports where sensing for Groups 1 and 2 ions occurs through the ether oxygen atoms in the lower rims of the calixarenes [42,43,46–50]. Membranes containing compound **1b**, with the *para*-quinone moiety, were found to reversibly vary in potential as the concentration of ions were varied, indicating that the

Table 1
Results from polymer membrane ion-selective electrode experiments with varying membrane compositions and Group 1 ions.

Ion (i)	Membrane composition	Slope of plot of E vs. $\log a_i/mV$	Linear concentration range/M
Cs ⁺	1a , KTBPB, PVC/NPOE	59.3	4.6×10^{-6} to 3.6×10^{-2}
Cs ⁺	1a , KTBPB, PVC/DBS	56.0	5.5×10^{-6} to 4.0×10^{-2}
Cs ⁺	1a , KTBPB, PVC/DOPP	52.9	4.5×10^{-6} to 1.1×10^{-2}
Cs ⁺	1a , KTBPB, PVC/DBP	56.0	3.6×10^{-6} to 4.0×10^{-2}
K ⁺	1a , KTBPB, PVC/NPOE	55.6	3.2×10^{-6} to 3.3×10^{-2}
Na ⁺	1a , KTBPB, PVC/NPOE	46.0	7.6×10^{-6} to 9.1×10^{-2}
Li ⁺	1a , KTBPB, PVC/NPOE	46.0	1.7×10^{-6} to 7.3×10^{-2}
Cs ⁺	1b , KTBPB, PVC/NPOE	56.9	4.6×10^{-6} to 4.0×10^{-2}
Cs ⁺	5a , KTBPB, PVC/NPOE	56.7	5.0×10^{-6} to 4.2×10^{-2}
Cs ⁺	5b , KTBPB, PVC/NPOE	59.9	5.0×10^{-6} to 4.3×10^{-2}
Cs ⁺	5c , KTBPB, PVC/NPOE	58.6	4.9×10^{-6} to 4.1×10^{-2}

presence of a phenolic group was not essential for a reversible response. Calixarenes containing phenolic groups [44,45] often display similar sensing properties to those without phenolic groups that interact with metal ions through the ether oxygen atoms [42,43,46–50]. Therefore, an explanation for compound **2a** not displaying ion-sensing properties may relate to solubility problems within the PVC membrane making it less mobile. Alternatively, **2a** is known to be not as chemically stable as the other compounds [10]. Thus, cations may act as Lewis acids and, by coordinating to C=O, may favour the decomposition (by de-bromination or de-*tert*-butylation) of the *p*-bromodienone system.

It was found that compounds **1a**, **1b**, **5a**, **5b** and **5c** all showed the highest selectivity for Cs⁺ compared to the other metal ions. There have been a number of reports where calix[4]arenes or calix[6]arenes have been found to be selective for Cs⁺ when incorporated into the polymer membranes of ion-selective electrodes [42–50]. Table 1 provides a summary of the sensing results obtained for the different compounds in the presence of different Group 1 ions as well as with different plasticizers in the membranes. In most instances the slopes were close to +59 mV (except for Na⁺ and Li⁺) and the linear region of the response was between 10^{-6} M and 10^{-2} M. The best result (in terms of the Nernstian slope) was obtained using NPOE as the plasticizer.

Table 2 gives selectivity coefficient results that were obtained from *p*-*t*-butylphenolic **1a** in the presence of a range of Groups 1 and 2 ions (and NH₄⁺) using the SSM and FIM methods [33]. Variations were obtained for the absolute selectivity coefficient values for the different ions using the different methods (FIM and SSM), but the trends were similar. It can be observed from the results in Table 2 that the ISE containing **1a** is more selective in the order Cs⁺ (0.25) > Rb⁺ (0.25) > K⁺ (0.3) > NH₄⁺ (0.25) > Na⁺ (0.43) > Li⁺ (0.6) > Ca²⁺ (0.6) > Mg²⁺ (0.8), which closely follows the order of hydrated ion size given in parenthesis (in nm) [51]. The selectivity for **1a** (and the other compounds) for Cs⁺ was similar to the selectivity observed from reports of other calix[4]arenes or calix[6]arenes, which suffer from the strongest interference from Rb⁺, K⁺ and NH₄⁺ [42–50]. Similarly, the relatively high Cs⁺/Na⁺

and Cs⁺/Li⁺ selectivity is comparable with other calix[4]arenes and calix[6]arenes [42–50].

4. Conclusions

The electrochemical oxidation of calix[4]arenes **5a**, **5b** and **5c** that contain a *p*-substituted phenolic group in the macrocyclic structure occurred by one-electron per molecule in dichloromethane on short voltammetric timescales (seconds) to most likely form cation radicals. In acetonitrile, and over the longer timescales (minutes to hours) of controlled potential electrolysis experiments, the cation radicals deprotonate to form neutral radicals which are further oxidised to reactive diamagnetic cations in an ECE mechanism. Compound **1b**, containing a quinone group in the macrocyclic structure displayed electrochemical properties similar to other quinones, that is, could be electrochemically reduced to a semiquinone in a one-electron reduction process at negative potentials.

With the exception of *p*-bromodienone **2a**, all of the compounds displayed ion-sensing properties for Groups 1 and 2 metals, with the highest selectivity shown for the Cs⁺ ion. The reason that **2a** did not potentiometrically respond to the cations most likely relates to chemical instability of **2a** or poor solubility (hence mobility) of **2a** within the PVC membrane. There appeared to be little change to the sensing properties by changing the quinone (**1b**) to a phenol (**1a**, **5a**, **5b** and **5c**) functionality, suggesting that the size of the macrocyclic structure was the most important factor in determining the sensing properties. Correspondingly, the order of selectivity of the Groups 1 and 2 ions (and NH₄⁺) calculated according to both the separate solution and fixed interference methods, were found to correlate with the order of the hydrated ion size.

Acknowledgment

This work was supported by a Singapore Government Ministry of Education research grant (T208B1222).

References

- [1] D. Diamond, M.A. McKervey, Chem. Soc. Rev. 25 (1996) 15.
- [2] D. Diamond, K. Nolan, Anal. Chem. 73 (2001) 22A.
- [3] R.M. El Nashar, H.A.A. Wagdy, H.Y. Aboul-Enein, Curr. Anal. Chem. 5 (2009) 249.
- [4] A. Ikeda, S. Shinkai, Chem. Rev. 97 (1997) 1713.
- [5] Z. Asfari, V. Böhmer, J. Harrowfield, J. Vicens (Eds.), Calixarenes 2001, Kluwer, Dordrecht, 2001.
- [6] J. Vicens, J. Harrowfield (Eds.), Calixarenes in the Nanoworld, Springer, Dordrecht, 2007.
- [7] C.D. Gutsche, Calixarenes: An Introduction, Royal Society of Chemistry, Cambridge, UK, 2008.
- [8] F. Troisi, T. Pierro, C. Gaeta, P. Neri, Org. Lett. 11 (2009) 697.
- [9] F. Troisi, T. Pierro, C. Gaeta, M. Carratù, P. Neri, Tetrahedron Lett. 50 (2009) 4416.
- [10] E. Wanigasekara, C. Gaeta, P. Neri, D.M. Rudkevich, Org. Lett. 10 (2008) 1263.
- [11] A. Pailleret, D.W.M. Arrigan, Electrochem. Commun. 3 (2001) 24.

Table 2
Ion selectivity coefficient measurements for Cs⁺ as the primary ion (i) in the presence of interfering ions (j) for a membrane composition of **1a**/KTBPB/PVC/NPOE.

Interfering ion (j)	\log_{10} selectivity coefficient ($\log_{10} K_{csj}^{pot}$)	
	SSM (from Eq. (2))	FIM (from Eq. (3))
Rb ⁺	−0.19	−0.58
K ⁺	−0.86	−1.65
NH ₄ ⁺	−1.26	−2.05
Na ⁺	−2.07	−2.65
Li ⁺	−2.64	−2.86
Ca ²⁺	−4.01	−3.81
Mg ²⁺	−4.49	−4.12

- [12] A. Pailleret, G. Herzog, D.W.M. Arrigan, *Electrochem. Commun.* 5 (2003) 68.
- [13] R. Vataj, A. Louati, C. Jeunesse, D. Matt, *J. Electroanal. Chem.* 565 (2004) 295.
- [14] G. Diao, J. Gu, *Electrochim. Acta* 52 (2006) 42.
- [15] O. Hammerich, B. Svensmark, in: H. Lund, M.M. Baizer (Eds.), *Organic Electrochemistry*, 3rd ed., Marcel Dekker, New York, 1991 (Chapter 16).
- [16] A. Rieker, R. Beisswenger, K. Regier, *Tetrahedron* 47 (1991) 645.
- [17] H. Eickhoff, G. Jung, A. Rieker, *Tetrahedron* 57 (2001) 353.
- [18] R.D. Webster, *Electrochem. Commun.* 1 (1999) 581.
- [19] U. Svanholm, K. Bechgaard, V.D. Parker, *J. Am. Chem. Soc.* 96 (1974) 2409.
- [20] L.L. Williams, R.D. Webster, *J. Am. Chem. Soc.* 126 (2004) 12441.
- [21] S.B. Lee, C.Y. Lin, P.M.W. Gill, R.D. Webster, *J. Org. Chem.* 70 (2005) 10466.
- [22] G.J. Wilson, C.Y. Lin, R.D. Webster, *J. Phys. Chem. B* 110 (2006) 11540.
- [23] S.B. Lee, A.C. Willis, R.D. Webster, *J. Am. Chem. Soc.* 128 (2006) 9332.
- [24] R.D. Webster, *Accounts Chem. Res.* 40 (2007) 251.
- [25] H.M. Peng, R.D. Webster, *J. Org. Chem.* 73 (2008) 2169.
- [26] W.W. Yao, H.M. Peng, R.D. Webster, *J. Phys. Chem. B* 112 (2008) 6847.
- [27] H.M. Peng, B.F. Choules, W.W. Yao, Z. Zhang, R.D. Webster, P.M.W. Gill, *J. Phys. Chem. B* 112 (2008) 10367.
- [28] W.W. Yao, H.M. Peng, R.D. Webster, *J. Phys. Chem. C* 113 (2009) 21805.
- [29] R.D. Webster, A.M. Bond, T. Schmidt, *J. Chem. Soc. Perkin Trans. 2* (1995) 1365.
- [30] E. Bakker, *J. Electrochem. Soc.* 143 (1996) L83.
- [31] E. Bakker, *Anal. Chem.* 69 (1997) 1061.
- [32] F.J.S. de Viteri, D. Diamond, *Analyst* 119 (1994) 749.
- [33] S. Makarychev-Mikhailov, A. Shvarev, E. Bakker, in: X. Zhang, H. Ju, J. Wang (Eds.), *Electrochemical Sensors, Biosensors and Their Biomedical Applications*, Academic Press, New York, 2007 (Chapter 4).
- [34] A.J. Bard, L.R. Faulkner, *Electrochemical Methods: Fundamentals and Applications*, 2nd ed., Wiley, New York, 2001.
- [35] A.M. Bond, T.L.E. Henderson, D.R. Mann, T.F. Mann, W. Thormann, C.G. Zoski, *Anal. Chem.* 60 (1988) 1878.
- [36] P. Lehtovuori, H. Joela, *Phys. Chem. Chem. Phys.* 4 (2002) 1928.
- [37] N. Gupta, H. Linschitz, *J. Am. Chem. Soc.* 119 (1997) 6384.
- [38] J.Q. Chambers, in: Z. Rappoport, S. Patai (Eds.), *The Chemistry of the Quinonoid Compounds*, vol. II, Wiley, New York, 1988, p. 719 (Chapter 12).
- [39] M. Quan, D. Sanchez, M.F. Wasylkiw, D.K. Smith, *J. Am. Chem. Soc.* 129 (2007) 12847.
- [40] Y. Hui, E.L.K. Chng, C.Y.L. Chng, H.L. Poh, R.D. Webster, *J. Am. Chem. Soc.* 131 (2009) 1523.
- [41] Y. Hui, E.L.K. Chng, L.P.-L. Chua, W.Z. Liu, R.D. Webster, *Anal. Chem.* 82 (2010) 1928.
- [42] J.S. Kim, A. Ohki, R. Ueki, T. Ishizuka, T. Shimotashiro, S. Maeda, *Talanta* 48 (1999) 705.
- [43] H. Oh, E.M. Choi, H. Jeong, K.C. Nam, S. Jeon, *Talanta* 53 (2000) 535.
- [44] L. Chen, H. Ju, X. Zeng, X. He, Z. Zhang, *Anal. Chim. Acta* 447 (2001) 41.
- [45] R.K. Mahajan, M. Kumar, V. Sharma, I. Kaur, *Talanta* 58 (2002) 445.
- [46] M. Arvand-Barmchi, M.F. Mousavi, M.A. Zanjanchi, M. Shamsipur, S. Taghvaei, *Anal. Lett.* 35 (2002) 7673.
- [47] S. Jeon, H. Yeo, H.K. Lee, S.W. Ko, K.C. Nam, *Electroanalysis* 16 (2004) 472.
- [48] Y. Choi, H. Kim, J.K. Lee, S.H. Lee, H.B. Lim, J.S. Kim, *Talanta* 64 (2004) 975.
- [49] R. Bereczki, V. Csokai, A. Grün, I. Bitter, K. Tóth, *Anal. Chim. Acta* 569 (2006) 42.
- [50] A. Radu, S. Peper, C. Gonczy, W. Runde, D. Diamond, *Electroanalysis* 18 (2006) 1379.
- [51] D.A. Skoog, D.M. West, F.J. Holler, S.R. Crouch, *Fundamentals of Analytical Chemistry*, 8th ed., Thomson Brooks/Cole, Belmont, 2004, p. 274.